

# Multiuser Massive MIMO Uplink Performance with Mutual Coupling Effects

Ran Zi\*, Xiaohu Ge\*, Haichao Wang\*, Jing Zhang\* and Cheng-Xiang Wang<sup>†</sup>

\*Dept. Electronics & Information Engineering

Huazhong University of Science & Technology, Wuhan, China

Email: xhge@mail.hust.edu.cn

<sup>†</sup>Joint Research Institute for Signal and Image Processing,

School of Engineering & Physical Sciences,

Heriot-Watt University, Edinburgh, EH14 4AS, UK.

**Abstract**—A multiuser massive MIMO system with mutual coupling is investigated in finite-dimensional channel scenarios. The uplink ergodic achievable rate is analytically derived for a multiuser massive MIMO system equipped with a rectangular planar uniform antenna array at the base station (BS). Numerical results show that the mutual coupling effect reduces the uplink achievable rate of multiuser massive MIMO systems when the antenna distance decreases. But when the size of the antenna array is fixed, the uplink achievable rate increases with the growing of antenna number.

**Index Terms**—Massive MIMO; mutual coupling; multiuser MIMO; finite-dimensional channel.

## I. INTRODUCTION

Over the last decade, the cellular system throughput and reliability have been greatly improved due to the application of MIMO technology. In order to satisfy the user's requirement on the growing transmission rate, utilizing the large-scale antenna array, or massive MIMO, is considered as a promising method to further improve the spectral efficiency in future 5G communication systems. Compared with conventional MIMO systems, the massive MIMO system integrated at the base station (BS) consists of hundreds of antennas, simultaneously serving dozens of user terminals [1], [2]. Previous studies have proved that the massive MIMO system could achieve the spectral efficiency up to 10-20bit/s/Hz and improve the energy efficiency even when using simple linear precoding algorithms [3]. However, in practical massive MIMO antenna arrays, due to the limit of array size and the large number of antennas, the distance between adjacent antennas is usually less than half a wavelength. In this case, the mutual coupling effect is very severe and the favorable propagation condition cannot be satisfied strictly, which greatly affects the performance of the massive MIMO communication systems [1], [4]. Therefore, it is important to analyze the impact of the mutual coupling effect on massive MIMO systems.

The mutual coupling effect was widely studied in the topic of antenna propagation [5], [6]. With the emerging of multi-antenna technology in wireless communications, the mutual coupling effect was also studied in wireless communications [7]–[9]. Based on the scattering parameter matrix, a matching network was introduced and a closed-form capacity expression

of the MIMO system with mutual coupling was derived in [7]. The impact of matching network on the bandwidth of antenna arrays was further investigated in [8]. At the subscriber unit on  $2 \times 2$  MIMO channels, the impact of mutual coupling induced by two closed spaced minimum scattering antennas was investigated in [9]. Moreover, for broadband systems with uniform circular arrays, a unified framework was presented to evaluate diversity limits of coupled broadband systems with varying antenna spacing [10]. However, the above studies were based on traditional MIMO systems, i.e. the number of transmitting and receiving antennas is less than  $8 \times 8$ . In massive MIMO systems employing hundreds of antennas at the BS, the mutual coupling effect on wireless communications was explored in recent literatures [11], [12]. It was demonstrated that the mutual coupling effect has practical limits on the spectrum efficiency of multiuser massive MIMO systems equipped with a 2-D square lattice array [11]. But only the impact of mutual coupling on the downlink SINR was investigated by the traditional Kronecher model in [11]. Considering mutual coupling as well as the finite dimensional channel model [13], the performance of massive MIMO system with a uniform linear array (ULA) was analyzed in [12]. However the maximum antenna number was only 30 during simulation results. Therefore, the impact of mutual coupling on the multiuser massive MIMO systems with the antenna number up to several hundreds needs to be further investigated.

This paper studies the multiuser massive MIMO system with mutual coupling equipped with a rectangular antenna array. Comparing with the linear arrays, rectangular arrays and other planar arrays are more space-efficient because they contain more antennas in a fixed area. And for the simplicity of distances between antenna elements, the rectangular array is selected. A lower bound of the uplink achievable rate is analytically derived for massive MIMO systems with mutual coupling in the single-cell multiuser scenario. When the size of the antenna array is fixed, the impact of mutual coupling on the uplink achievable rates is analyzed by numerical results. These results provide some guidelines for designing suitable antenna numbers and distances in the fixed-size antenna array to optimize the uplink achievable rate for multiuser massive MIMO systems.

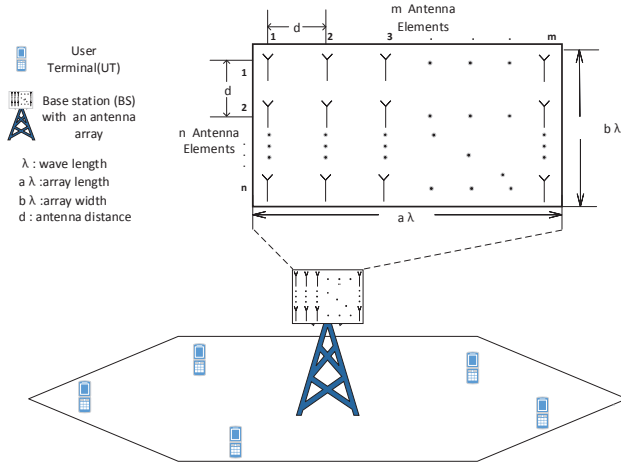


Fig. 1. System model.

The remainder of this paper is outlined as follows. Section II describes a system model for multiuser massive MIMO systems. In section III, the lower bound of uplink achievable rate is analytically derived in a finite dimensional channel scenario. Numerical results and discussions are presented in section IV. In the end, conclusions are drawn in section V.

## II. SYSTEM MODEL

As depicted in Fig. 1, we consider a scenario with multiusers uniformly located in a single cell. A BS equipped with  $M$  antennas simultaneously serves  $K$  active user terminals (UTs). Each UT has a single antenna, while  $M$  antennas integrated at the BS make up a rectangular uniform planar array. The size of the rectangular array is assumed as  $a\lambda \times b\lambda$ , where  $\lambda$  is the wavelength of the wireless signal,  $a$  and  $b$  are the length and width of the array, respectively. The distance between adjacent antennas is denoted as  $d$ . The number of antennas in each row and column is  $m$  and  $n$  respectively. Therefore we have  $d = \frac{a\lambda}{m-1} = \frac{b\lambda}{n-1}$  and  $M = mn$ .

### A. Signal and Channel Model

In this paper, we focus on uplinks of multiuser massive MIMO systems. The received uplink signal at a BS is expressed as

$$\mathbf{y} = \sqrt{SNR_{UT}} \mathbf{C} \mathbf{A} \mathbf{H} \mathbf{x} + \mathbf{w}, \quad (1)$$

where  $SNR_{UT}$  is the signal-to-noise ratio (SNR) at UTs,  $\mathbf{x} \in \mathbb{C}^{K \times 1}$  is a vector denoting the symbols simultaneously transmitted from  $K$  active UTs ( $\mathbb{C}^{M \times 1}$  refers to an  $M \times 1$  vector), and  $\mathbf{w} \in \mathbb{C}^{M \times 1}$  denotes the additive white Gaussian noise (AWGN) in wireless channels with zero mean and unit variance.  $\mathbf{C}$  is the  $M \times M$  mutual coupling matrix which represents the impact on the received signal caused by mutual coupling effects.  $\mathbf{A} \in \mathbb{C}^{M \times P}$  is the array steering matrix

denoting the limited number of incident directions in the finite-dimensional channels [12].  $\mathbf{H} \in \mathbb{C}^{P \times K}$  is the propagation response matrix standing for both small scale fading and large scale fading, which is expressed as

$$\mathbf{H} = [\mathbf{h}_1, \dots, \mathbf{h}_k, \dots, \mathbf{h}_K] \in \mathbb{C}^{P \times K}, \quad (2a)$$

with

$$\mathbf{h}_k = \beta_k^{1/2} [h_{k,1}, \dots, h_{k,q}, \dots, h_{k,P}]^T, \quad (2b)$$

where  $\beta_k$  is the large scale fading coefficient of the  $k$ th UT,  $h_{k,q}$  ( $1 \leq q \leq P$ ) is the complex small scale fading coefficient which corresponds to the  $q$ th incident direction transmitted from the  $k$ th UT. The small scale fading of different incident directions or different UTs is assumed to be subject to independent and identical Gaussian distributions with zero mean and unit variance, i.e.  $h_{k,q} \sim \mathcal{CN}(0, 1)$ .

### B. Modeling of Array Steering Matrix

In wireless systems employing massive MIMO, it may exceed the degree of freedom that the physical channel can offer if the antenna number keeps rising without bound [13]. The finite dimensional physical channel model is proposed to represent this phenomenon. In this model, the incident signals to the antenna array is divided into  $P$  finite directions in angular domain. In general, the larger value of  $P$  corresponds to the richer scattering environment around the BS.

Each independent incident direction has its identical azimuth angle  $\phi_q$  and elevation angle  $\theta_q$  ( $\phi_q \in [-\pi, \pi]$ ,  $\theta_q \in [-\pi/2, \pi/2]$ ,  $q = 1, \dots, P$ ). For the signal originating from the  $q$ th incident direction, its response on the antenna located at the  $c$ th row and  $e$ th column of the rectangular array ( $c = 1, \dots, n$ ;  $e = 1, \dots, m$ ) is denoted by

$$a_{ce}^q = \exp \left\{ j \frac{2\pi}{\lambda} [(c-1)d \cos \phi_q \sin \theta_q + (e-1)d \sin \phi_q \sin \theta_q] \right\}. \quad (3)$$

(3) is based on the assumption that the antenna located at the first row and first column is the reference point with zero phase response and the amplitude responses of all antennas are normalized as 1.

Therefore, the response of the  $q$ th incident direction on the whole array containing  $M$  antennas is denoted by

$$\mathbf{a}(\phi_q, \theta_q) = [1, \dots, a_{ce}^q, \dots, a_{nm}^q]^T \in \mathbb{C}^{M \times 1}. \quad (4)$$

Considering all  $P$  independent incident directions, the  $M \times P$  array steering matrix of the whole array is given by

$$\mathbf{A} = [\mathbf{a}(\phi_1, \theta_1), \dots, \mathbf{a}(\phi_q, \theta_q), \dots, \mathbf{a}(\phi_P, \theta_P)] \in \mathbb{C}^{M \times P}. \quad (5)$$

### C. Modeling of Mutual Coupling

The mutual coupling matrix  $\mathbf{C} \in \mathbb{C}^{M \times M}$  is expressed as [9]

$$\mathbf{C} = Z_L (Z_L \mathbf{I}_M + \mathbf{Z}_C)^{-1}, \quad (6)$$

where  $Z_L$  is the load impedance which is assumed to be constant for all antenna elements.  $\mathbf{I}_M$  is an  $M \times M$  unit matrix and  $\mathbf{Z}_C$  is the  $M \times M$  mutual impedance matrix. According to

the rectangular antenna array in Fig. 1, the mutual impedance matrix  $\mathbf{Z}_C$  can be constituted by  $n \times n$  sub-matrices, i.e.,  $\mathbf{Z}_C = [\mathbf{Z}_{st}]_{n \times n}$ . The sub-matrix  $\mathbf{Z}_{st}$  is an  $m \times m$  mutual impedance matrix consists of the mutual impedances between the  $m$  antennas at the  $s$ th ( $s = 1, \dots, n$ ) row and the  $m$  antennas at the  $t$ th ( $t = 1, \dots, n$ ) row in the rectangular antenna array.  $\mathbf{Z}_{st}$  is expressed as

$$\mathbf{Z}_{st} = \begin{bmatrix} z_{11}^{st} & z_{12}^{st} & \dots & z_{1m}^{st} \\ z_{21}^{st} & z_{22}^{st} & \dots & z_{2m}^{st} \\ \vdots & \vdots & \ddots & \vdots \\ z_{m1}^{st} & z_{m2}^{st} & \dots & z_{mm}^{st} \end{bmatrix}, \quad (7)$$

where  $z_{uv}^{st}$  is the mutual impedance between  $Ant_{su}$  and  $Ant_{tv}$ .  $Ant_{su}$  refers to the antenna located at the  $s$ th row and  $u$ th column ( $u = 1, \dots, m$ ) of the rectangular array;  $Ant_{tv}$  refers to the antenna located at the  $t$ th row and  $v$ th column ( $v = 1, \dots, m$ ). Furthermore, the distance between  $Ant_{su}$  and  $Ant_{tv}$  is expressed as  $d_{uv}^{st} = d\sqrt{(t-s)^2 + (v-u)^2}$ . Therefore, the mutual impedance  $z_{uv}^{st}$  can be calculated based on results in [9]. Since the calculation is quite straight forward, we omit the detailed expression of  $z_{uv}^{st}$  here.

Assuming that all the array elements are the same, the mutual impedance  $z_{uv}^{st}$  only depends on the distance between antennas. Since the distance between adjacent antennas remains unchanged in the uniform array, the following properties are obtained as

$$z_{uv}^{st} = z_{(u+1),(v+1)}^{st}, \quad (8a)$$

$$z_{uv}^{st} = z_{vu}^{st}. \quad (8b)$$

Furthermore, similar properties for the matrix  $\mathbf{Z}_{st}$  are derived as

$$\mathbf{Z}_{st} = \mathbf{Z}_{(s+1),(t+1)}, \quad (9a)$$

$$\mathbf{Z}_{st} = \mathbf{Z}_{ts}. \quad (9b)$$

According to (7), (8) and (9), the  $M \times M$  mutual impedance matrix  $\mathbf{Z}_C$  is derived by calculating  $M$  entries in the first row of the mutual impedance matrix. If there are hundreds of antennas located in the antenna array, this is a much more convenient and efficient way to obtain  $\mathbf{Z}_C$  than calculating all mutual impedances directly. As a consequence, the mutual coupling matrix  $\mathbf{C}$  can be derived from (6).

### III. ACHIEVABLE RATES

In Section II, we have first derived all parameters in (1). Furthermore, we try to investigate the uplink achievable rate, which considers mutual coupling as well as the finite dimensional channel.

The whole channel gain is denoted as  $\mathbf{G} = \mathbf{CAH} = [\mathbf{g}_1, \dots, \mathbf{g}_k, \dots, \mathbf{g}_K]$  which is acquired via perfect channel estimation. Then we utilize a conventional linear detecting scheme, i.e., maximum-ratio combining (MRC) scheme, to estimate the received signal. The estimated signal vector after the MRC detector is expressed as

$$\tilde{\mathbf{y}} = \mathbf{G}^\dagger \mathbf{y} = \sqrt{SNR_{UT}} \mathbf{G}^\dagger \mathbf{G} \mathbf{x} + \mathbf{G}^\dagger \mathbf{w}. \quad (10)$$

Furthermore, the estimated symbol from the  $k$ th UT is extended as

$$\tilde{y}_k = \sqrt{SNR_{UT}} \mathbf{g}_k^\dagger \mathbf{g}_k x_k + \sqrt{SNR_{UT}} \sum_{l=1, l \neq k}^K \mathbf{g}_k^\dagger \mathbf{g}_l x_l + \mathbf{g}_k^\dagger \mathbf{w}, \quad (11)$$

where  $\mathbf{g}_k$  and  $\mathbf{g}_l$  are the channel vectors of the  $k$ th and  $l$ th UT respectively, as given by

$$\mathbf{g}_k = \mathbf{CAh}_k, \mathbf{g}_l = \mathbf{CAh}_l. \quad (12)$$

Considering the independence between  $\mathbf{h}_k$  and  $\mathbf{h}_l$ ,  $\mathbf{g}_k$  and  $\mathbf{g}_l$  are independent from each other as well.

After signal detection, the SINR at the BS is expressed as

$$SINR_{BS} = \frac{SNR_{UT} |\mathbf{g}_k^\dagger \mathbf{g}_k|^2}{SNR_{UT} \sum_{l=1, l \neq k}^K |\mathbf{g}_k^\dagger \mathbf{g}_l|^2 + \|\mathbf{g}_k^\dagger\|^2}. \quad (13)$$

Based on the Shannon theorem, the ergodic uplink achievable rate of the  $k$ th UT is derived by

$$R_k = \mathbb{E} \left[ \log_2 \left( 1 + \frac{SNR_{UT} |\mathbf{g}_k^\dagger \mathbf{g}_k|^2}{SNR_{UT} \sum_{l=1, l \neq k}^K |\mathbf{g}_k^\dagger \mathbf{g}_l|^2 + \|\mathbf{g}_k^\dagger\|^2} \right) \right]. \quad (14)$$

Based on the convexity of  $\log_2(1 + \frac{1}{x})$  and Jensen's inequality [13], we have

$$R_k \geq \log_2 \left\{ 1 + \left[ \mathbb{E} \left( \frac{SNR_{UT} \sum_{l=1, l \neq k}^K |\mathbf{g}_k^\dagger \mathbf{g}_l|^2 + \|\mathbf{g}_k^\dagger\|^2}{SNR_{UT} |\mathbf{g}_k^\dagger \mathbf{g}_k|^2} \right) \right]^{-1} \right\}. \quad (15)$$

We set the determinate matrix  $\mathbf{F} = \mathbf{CA}$ . According to the singular value decomposition,  $\mathbf{F} = \mathbf{U}\mathbf{\Sigma}\mathbf{V}^\dagger$  is extended, where  $\mathbf{U}$  and  $\mathbf{V}$  are an  $M \times M$  unitary matrix and a  $P \times P$  unitary matrix, respectively, and  $\mathbf{\Sigma} = \begin{pmatrix} \mathbf{\Delta} & \mathbf{0} \\ \mathbf{0} & \mathbf{0} \end{pmatrix}$  is an  $M \times P$  matrix, with  $\mathbf{\Delta}$  being an  $r \times r$  diagonal matrix whose none-zero entries  $\varepsilon_1, \varepsilon_2, \dots, \varepsilon_r$  are singular values of  $\mathbf{F}$ . Furthermore, the term  $|\mathbf{g}_k^\dagger \mathbf{g}_l|$  is derived as

$$\begin{aligned} |\mathbf{g}_k^\dagger \mathbf{g}_l| &= |\mathbf{h}_k^\dagger \mathbf{V} \mathbf{\Sigma}^\dagger \mathbf{U}^\dagger \mathbf{U} \mathbf{\Sigma} \mathbf{V}^\dagger \mathbf{h}_l| \\ &= \text{Trace}(\mathbf{h}_k \mathbf{h}_k^\dagger \mathbf{\Sigma}^\dagger \mathbf{\Sigma}) = \sum_{i=1}^r \varepsilon_i^2 h_{l,i} h_{k,i}^\dagger. \end{aligned} \quad (16)$$

Substituting (16) into (15), the expectation term in (15) is derived as

$$\begin{aligned}
 & \mathbb{E} \left( \frac{SNR_{UT} \sum_{l=1, l \neq k}^K |\mathbf{g}_k^\dagger \mathbf{g}_l|^2 + \|\mathbf{g}_k^\dagger\|^2}{SNR_{UT} |\mathbf{g}_k^\dagger \mathbf{g}_k|^2} \right) \\
 &= \sum_{l=1, l \neq k}^K \mathbb{E} \left( \frac{\left( \sum_{i=1}^r \varepsilon_i^2 h_{l,i} h_{k,i}^\dagger \right)^2}{\left( \sum_{i=1}^r \varepsilon_i^2 h_{k,i} h_{k,i}^\dagger \right)^2} \right) \\
 & \quad + \frac{1}{SNR_{UT}} \mathbb{E} \left( \frac{\sum_{i=1}^r \varepsilon_i^2 |h_{k,i}|^2}{\left( \sum_{i=1}^r \varepsilon_i^2 |h_{k,i}|^2 \right)^2} \right), \quad (17) \\
 & \stackrel{(a)}{=} \left( \sum_{l=1, l \neq k}^K \beta_l \right) \left( \sum_{i=1}^r \varepsilon_i^4 \right) \mathbb{E} \left( \frac{\sum_{i=1}^r |h_{k,i}|^2}{\left( \sum_{i=1}^r \varepsilon_i^2 |h_{k,i}|^2 \right)^2} \right) \\
 & \quad + \frac{1}{SNR_{UT}} \mathbb{E} \left( \frac{1}{\sum_{i=1}^r \varepsilon_i^2 |h_{k,i}|^2} \right)
 \end{aligned}$$

where (a) is obtained based on the independence between  $h_{l,i}$  and  $h_{k,i}$ , and  $h_{l,i}, h_{k,i} \sim \mathcal{CN}(0, 1)$ . According to the Chebyshev's inequality expressed as 11.115 in [15], we can write

$$\sum_{l=1}^r \varepsilon_l^2 |h_{k,i}|^2 \geq \frac{1}{r} \sum_{l=1}^r \varepsilon_l^2 \sum_{l=1}^r |h_{k,i}|^2. \quad (18)$$

Combining (18) with (17), we derive (19) at the top of the next page, where (b) is obtained via the property of Wishart matrix [16] expressed as

$$\mathbb{E} \left( \frac{1}{\sum_{i=1}^r |h_{k,i}|^2} \right) = \mathbb{E} [\text{tr}(\mathbf{W}^{-1})] = \frac{1}{\beta_k (r-1)}, \quad (20)$$

with  $\mathbf{W} = \mathbf{h}_{k,i}^\dagger \mathbf{h}_{k,i}$ , which is a  $1 \times 1$  Wishart matrix. Substituting (17) and (19) into (15), the analytical expression of the lower bound of the uplink ergodic achievable rate for the  $k$ th UT is derived as (21), which is below (19) on the next page. Moreover, the lower bound for the total achievable rate for all  $K$  UTs is denoted by  $\tilde{R} = \sum_{k=1}^K \tilde{R}_k$ .

#### IV. NUMERICAL RESULTS AND DISCUSSION

In this section the proposed lower bound of the ergodic achievable rate for all UTs are numerically simulated. The impact of the mutual coupling effect on multiuser massive MIMO systems is analyzed considering the finite-dimensional channel. In the following analysis, some default parameters are configured: the ratio of the length and width of the rectangular antenna array is set as  $a/b = 2$ , the type of antennas is the

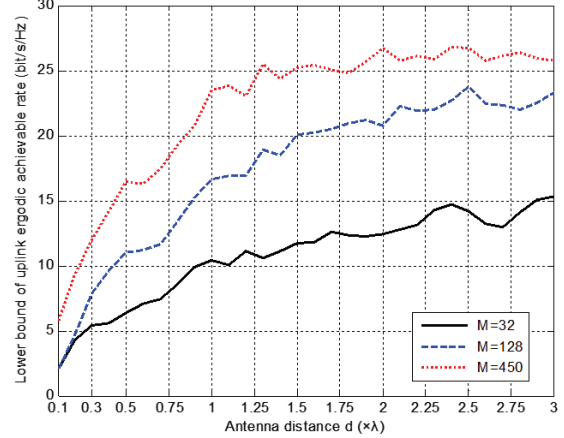


Fig. 2. Lower bound of uplink ergodic achievable rate with respect to the antenna distance considering different antenna numbers.

dipole antenna whose length is  $0.5\lambda$ , the load impedance  $Z_L$  at every antenna is 50 ohms [12], the large scale fading factor for each UT is reasonably normalized as 1 for simplicity [13], the transmit SNR at the UT is 10dB, and the number of the incident direction  $P$  is set as 70.

The lower bound of uplink ergodic achievable rate for all UTs with respect to the antenna distance considering different antenna numbers is illustrated in Fig. 2. When the antenna number is fixed, the lower bound of uplink ergodic achievable rate increases with the increasing of the antenna distance. This is consistent with the results in [9] that the larger antenna distance leads to the smaller correlation which leads to higher capacity. The fluctuation of curves is due to the up-and-down of the mutual impedance when antenna distance increases [14]. When the antenna distance is fixed, the larger antenna number leads to the larger achievable rate.

Fig. 3 shows the total uplink achievable rates for all UTs rise with the growing of antenna number when antenna distance is fixed. Meanwhile, the larger antenna distance corresponds to the higher achievable rate. But the gap between the two curves of  $0.8\lambda$  and  $0.5\lambda$  is smaller than that between the two of  $0.5\lambda$  and  $0.2\lambda$ . This is also consistent with the phenomenon in Fig. 2 where the rising rate of the achievable rates slows down when the antenna distance increases.

When the array size is fixed, the lower bound of uplink ergodic achievable rate for all UTs with respect to the antenna distance is investigated in Fig. 4. Without loss of generality, the size of the antenna array is fixed as  $6\lambda \times 3\lambda$ . In the fixed-size array, a tradeoff exists between the antenna distance and the antenna number, since the increasing antenna distance leads to the decreasing antenna number. As shown in Fig. 4, no matter the mutual coupling or limited incident directions are considered or not, the lower bound of uplink ergodic achievable rate decreases with the increasing of antenna distance. When the number of incident directions  $P$  is

$$\begin{aligned}
 & \left( \sum_{l=1, l \neq k}^K \beta_l \right) \left( \sum_{i=1}^r \varepsilon_i^4 \right) \mathbb{E} \left( \frac{\sum_{i=1}^r |h_{k,i}|^2}{\left( \sum_{i=1}^r \varepsilon_i^2 |h_{k,i}|^2 \right)^2} \right) + \frac{1}{SNR_{UT}} \mathbb{E} \left( \frac{1}{\sum_{i=1}^r \varepsilon_i^2 |h_{k,i}|^2} \right) \\
 & \leq \left( \sum_{l=1, l \neq k}^K \beta_l \right) \left( \sum_{i=1}^r \varepsilon_i^4 \right) \mathbb{E} \left( \frac{r^2 \sum_{i=1}^r |h_{k,i}|^2}{\left( \sum_{i=1}^r \varepsilon_i^2 \right)^2 \left( \sum_{i=1}^r |h_{k,i}|^2 \right)^2} \right) + \frac{1}{SNR_{UT}} \mathbb{E} \left( \frac{r}{\left( \sum_{i=1}^r \varepsilon_i^2 \right) \left( \sum_{i=1}^r |h_{k,i}|^2 \right)} \right) \\
 & = \frac{r^2 \text{Trace} \left( (\mathbf{F}^\dagger \mathbf{F})^2 \right) \left( \sum_{l=1, l \neq k}^K \beta_l \right)}{\left( \text{Trace}(\mathbf{F}^\dagger \mathbf{F}) \right)^2} \mathbb{E} \left( \frac{1}{\sum_{i=1}^r |h_{k,i}|^2} \right) + \frac{r}{SNR_{UT} \left( \text{Trace}(\mathbf{F}^\dagger \mathbf{F}) \right)} \mathbb{E} \left( \frac{1}{\left( \sum_{i=1}^r |h_{k,i}|^2 \right)} \right) \\
 & \stackrel{(b)}{=} \frac{r^2 SNR_{UT} \text{Trace} \left( (\mathbf{F}^\dagger \mathbf{F})^2 \right) \left( \sum_{l=1, l \neq k}^K \beta_l \right) + r \text{Trace}(\mathbf{F}^\dagger \mathbf{F})}{\beta_k (r-1) SNR_{UT} \left( \text{Trace}(\mathbf{F}^\dagger \mathbf{F}) \right)^2} \\
 & R_k \geq \tilde{R}_k = \log_2 \left\{ 1 + \frac{\beta_k (r-1) SNR_{UT} \left( \text{Trace}(\mathbf{F}^\dagger \mathbf{F}) \right)^2}{r^2 SNR_{UT} \left( \sum_{l=1, l \neq k}^K \beta_l \right) \text{Trace} \left( (\mathbf{F}^\dagger \mathbf{F})(\mathbf{F}^\dagger \mathbf{F}) \right) + r \text{Trace}(\mathbf{F}^\dagger \mathbf{F})} \right\}
 \end{aligned} \tag{19}$$

$$\tag{21}$$

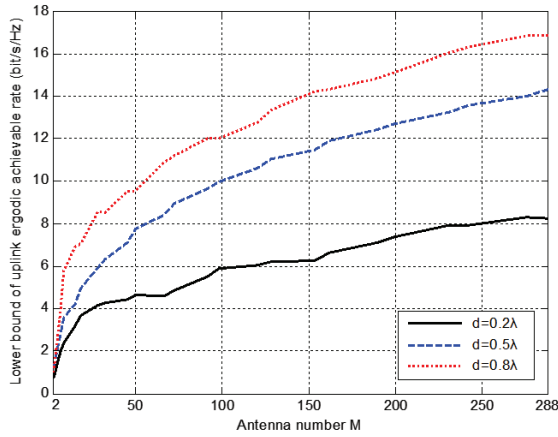


Fig. 3. Lower bound of uplink ergodic achievable rate with respect to the antenna number considering different antenna distances.

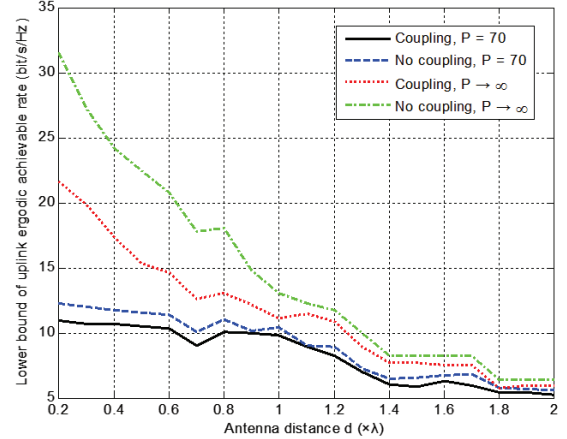


Fig. 4. Lower bound of uplink ergodic achievable rate with respect to the antenna distance while the array size is fixed.

fixed as 70, the lower bound of uplink ergodic achievable rate with mutual coupling is less than that with no mutual coupling. When  $P$  approaches infinity, the lower bound of uplink ergodic achievable rate with mutual coupling is also less than that with no mutual coupling. Fig. 4 illustrates both the mutual coupling and limited incident directions in the finite-dimensional channel have a negative impact on the achievable rate.

In Fig. 5, the lower bound of uplink ergodic achievable

rate for all UTs with respect to the increasing number of UTs is investigated while the antenna array is fixed. The size of the antenna array is fixed as  $6\lambda \times 3\lambda$ . The antenna distance is fixed as  $0.38\lambda$  and antenna number is fixed as 128. Fig. 5 illustrates that the lower bound of the uplink ergodic achievable rate for all UTs increases when the number of UTs increases. When the number of incident directions  $P$  is fixed as 70, the lower bound of the uplink ergodic achievable rate with mutual coupling is below that without mutual coupling.

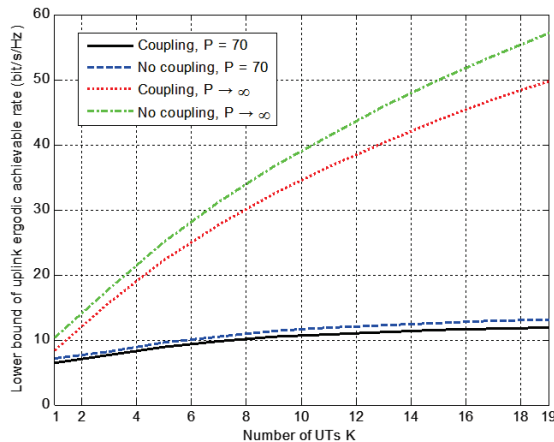


Fig. 5. Lower bound of uplink ergodic achievable rate with respect to the number of UTs while the antenna array is fixed.

And when  $P$  approaches infinity, the lower bound of the uplink ergodic achievable rate is also less than that without mutual coupling. This conforms with the finding in Fig. 4 that both mutual coupling and limited incident directions have an adverse impact on the achievable rate.

## V. CONCLUSION

In this paper, the impact of mutual coupling effect on multiuser massive MIMO systems employing a rectangular uniform planar antenna array is investigated. Moreover, a lower bound of the uplink ergodic achievable rate has been analytically derived for a multiuser massive MIMO system. In the finite-dimensional channel scenarios, numerical results show that the mutual coupling and limited incident directions reduce the achievable rate in multiuser massive MIMO systems, especially when the antenna distance is small or the number of UTs is large. In a fixed-size rectangular array, where the antenna distance and the antenna number change simultaneously, the achievable rate increases with the growing of antenna number in multiuser massive MIMO systems. In the future, we will explore the new conformal antenna array and the new precoding and detection schemes to reduce the negative impact of mutual coupling on the multiuser massive MIMO systems.

## ACKNOWLEDGMENT

R. Zi, X. Ge (corresponding author), H. Wang and J. Zhang would like to acknowledge the support from the Ministry of Science and Technology (MOST) of China under the grants 2014DFA11640, 2012DFG12250 and 0903, the National Natural Science Foundation of China (NSFC) under the grants 61271224, the NFSC Major International Joint Research Project under the grant 61210002, the Hubei Provincial Science and Technology Department under the grant 2011BFA004 and 2013BHE005, and the Fundamental Research Funds for the Central Universities under the

grant 2013QN136, 2014TS100 and 2014QN155. This research is partially supported by EU FP7-PEOPLE-IRSES, project acronym S2EuNet (grant no. 247083), project acronym WiNDOW (grant no. 318992) and project acronym CROWN (grant no. 610524).

## REFERENCES

- [1] F. Rusek, D. Persson and B. K. Lau, "Scaling up MIMO: opportunities and challenges with very large arrays," *IEEE Signal Process. Mag.*, vol. 30, no. 1, pp. 40–60, Jan. 2013.
- [2] T. L. Marzetta, "Noncooperative cellular wireless with unlimited numbers of base station antennas," *IEEE Trans. Wireless Commun.*, vol. 9, no. 11, pp. 3590–3600, Nov. 2010.
- [3] H. Q. Ngo, E. G. Larsson and T. L. Marzetta, "Energy and spectral efficiency of very large multiuser MIMO systems," *IEEE Trans. Commun.*, vol. 61, no. 4, pp. 1436–1449, April 2013.
- [4] Z. Xu, S. Sfar and R. Blum, "Receive antenna selection for closely-spaced antennas with mutual coupling," *IEEE Trans. Wireless Commun.*, vol. 9, no. 2, pp. 652–661, Feb. 2010.
- [5] H. Steyskal and J. S. Herd, "Mutual coupling compensation in small array antennas," *IEEE Trans. Antennas and Propag.*, vol. 38, no. 12, pp. 1971–1975, Dec. 1990.
- [6] T. Svantesson and A. Ranheim, "Mutual coupling effects on the capacity of multielement antenna systems," in *Proc. IEEE ICASSP'01*, May 2001, pp. 2485–2488.
- [7] J. W. Wallace and M. A. Jensen, "Mutual coupling in MIMO wireless systems: a rigorous network theory analysis," *IEEE J. Select. Areas Commun.*, vol. 3, no. 4, pp. 1317–1325, July 2004.
- [8] B. L. Lau, J. Bach Andersen, G. Kristensson and A. F. Molisch, "Impact of matching network on bandwidth of compact antenna arrays," *IEEE Trans. Antennas Propag.*, vol. 54, no. 11, pp. 3225–3238, Nov. 2006.
- [9] B. Clerckx, C. Craeye, D. Vanhoenacker-Janvier and C. Oestges, "Impact of antenna coupling on 2 x 2 MIMO communications," *IEEE Trans. Veh. Technol.*, vol. 56, no. 3, pp. 1009–1018, May 2007.
- [10] P. S. Taluja and L. H. Brian, "Diversity limits of compact broadband multi-antenna systems," *IEEE J. Select. Areas Commun.*, vol. 31, no. 2, pp. 326–337, Feb. 2013.
- [11] X. Artiga, B. Devillers, and J. Perruisseau-Carrier, "Mutual coupling effects in multi-user massive MIMO base stations," in *Proc. IEEE APSURSI'7*, July 2012, pp. 1–2.
- [12] C. Masouros, M. Sellathurai, and T. Ratnarajah, "Large-scale MIMO transmitters in fixed physical spaces: the effect of transmit correlation and mutual coupling," *IEEE Trans. Commun.*, vol. 61, no. 7, pp. 2794–2804, July 2013.
- [13] H. Q. Ngo, E. Larsson and T. Marzetta, "The multicell multiuser MIMO uplink with very large antenna arrays and a finite-dimensional channel," *IEEE Trans. Commun.*, vol. 61, no. 6, pp. 2350–2361, June 2013.
- [14] C. A. Balanis, *Antenna Theory: Analysis and Design*. John Wiley and Sons, 2012.
- [15] I. S. Gradshteyn and I. M. Ryzhik, *Table of integrals, series, and products*. Academic Press, 2007.
- [16] A. M. Tulino and S. Verdú, "Random matrix theory and wireless communications," *Foundations Trends Commun. Inf. Theory*, vol. 1, no. 1, pp. 1–182, June 2004.